Establishing Optimal Wave Communication Channels Automatically

David A. B. Miller, *Fellow, IEEE*

***Abstract*—We show how multiple optimal orthogonal channels for communicating or interconnecting with waves between two objects can be aligned and optimized automatically using controllable beamsplitters, detectors and simple local feedback loops, without moving parts, without device calibration, without fundamental beam splitting loss, and without calculations. Optical applications include multiple simultaneous orthogonal spatial communication channels in free space or multimode optical fibers, automatically focused power delivery with waves, multiple channel communication through scattering or lossy media, and real-time-optimized focused channels to and from multiple moving objects. The approach physically implements automatic singular value decomposition of the wave coupling between the objects, and is equivalent in its effect to the beam forming in a laser resonator with phase-conjugate mirrors with the additional benefits of allowing multiple orthogonal channels to be formed simultaneously and avoiding the need for any nonlinear optical materials.**

***Index Terms*—Communications channels, matrix decomposition, optical interconnections, optical phase conjugation, optical planar waveguide couplers, optical propagation in nonhomogeneous media.**

I. Introduction

ESTABLISHING optimal interconnections, communication channels, or beams with waves is of obvious importance in many applications in electromagnetics [1]–[11] and acoustics [12], including remote or biomedical [11], [12] sensing, and wireless [1]–[4] or optical [8], [10] communications. For example, present increasing demands for telecommunication capacity are forcing the consideration of spatial degrees of freedom in multimode optical fibers so as to provide more orthogonal communication channels [10]. Self-aligning channels are of obvious usefulness in free-space communications or interconnects. One difficulty in fully exploiting multiple communication channels simultaneously is that there may be scattering between simple channels during propagation—for example, between the different spatial modes in an optical fiber or between simple beams when propagating through a scattering environment. There may also be different amounts of loss on different channels (i.e., nonunitary transmission), which generally means that orthogonal inputs do not guarantee orthogonal outputs.

Techniques are well-known in radio-frequency MIMO (multiple-input multiple-output) systems for optimizing transmission channels in multiple antenna systems [1]–[4], but these generally require knowledge and/or measurement of the transmission matrix between transmitting and receiving antennas. Optical schemes have similarly been devised based on equivalent prior measurements of the transmission matrix through some scattering object [5]–[10], though interferometric [5]–[9] or coherent detection [10] techniques are necessary because in optics we typically measure intensities rather than fields. Following such measurement of the transmission matrix, all those schemes [1]–[10] require extensive mathematical calculation to evaluate the necessary channels, with singular value decomposition (SVD) of the transmission matrix [13]–[15] being a well-known approach that optimizes power coupling in the resulting orthogonal channels. Optical phase conjugation can physically perform an optimization without prior measurements and calculations [16]–[19], but it can only find the most strongly coupled SVD channel and requires nonlinear optical materials that work in the power, wavelength, and response-time ranges of interest.

Optical multiple channel schemes generally have had a further challenge compared to radio-frequency systems, which is the difficulty of combining or separating channels losslessly. In radio-frequency systems, it is straightforward and routine to measure the input fields directly and then to separate channels by purely mathematical computational means. Similarly at the output, it is straightforward to add up the necessary combinations of signals mathematically and use the results to drive output antennas. In optics, other than for narrow bandwidths [10] using homodyne or heterodyne techniques, it is not generally possible to measure the optical input fields directly at the input. At the output, it is not clear if there is any optical apparatus that can generate an arbitrary optical wave from some desired computed form, even if that computation was possible at optical frequencies. As a result, optical beams generally need to be separated and combined physically, not computationally. It has not been clear until recently [20], however, how to combine or separate arbitrary orthogonal optical beams without substantial splitting or combining loss, restricting many other schemes to a single channel or to tolerating that loss [10]. A further issue with optical implementations based on measurement and calculation is that, even if we do measure the coupling operator and calculate a desired set of optical outputs, we have to carefully calibrate and stabilize the optical input and/or output devices so that we know the corresponding field amplitudes and phases being set by them; recent work on the relatively simple optical beamforming

Manuscript received June 3, 2013; accepted August 13, 2013. Date of publication August 14, 2013; date of current version November 27, 2013. This work was supported in part by the funds from Duke University under an award from DARPA InPho program and in part by Multidisciplinary University Research Initiative grants (Air Force Office of Scientific Research, FA9550-10-1-0264 and FA9550-09-0704). Portions of this work were completed while the author was a Carnegie Centenary Professor at Strathclyde University, supported by the Carnegie Trust for the Universities of Scotland.

The author is with the Ginzton Laboratory, Stanford University, Stanford, CA 94305-4088 USA (e-mail: dabm@ee.stanford.edu).

Color versions of one or more of the figures in this paper are available online at http://ieeexplore.ieee.org.

Digital Object Identifier 10.1109/JLT.2013.2278809

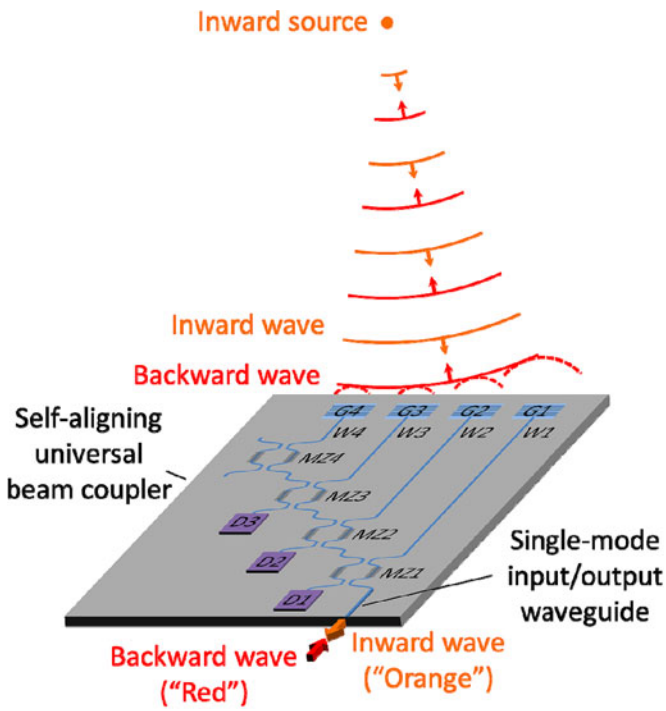

Fig. 1. Illustration of bidirectional optimized coupler. An inward wave is coupled through grating couplers (G1–G4) and waveguides (W1–W4) to Mach–Zehnder interferometers (MZ1–MZ4), with detectors (D1–D3) for feedback control of the modulators, to give a single-mode output of this inward wave from the single-mode input/output waveguide at the bottom right (thick orange arrow), as described in [20]. Then a backward wave (thick red arrow) sent in through the same waveguide will lead to a backward wave optimally focused back to the original source. The dashed lines indicate the waves coming from the grating couplers that, in the spirit of Huygens' wavelets [22], construct the backward waves focusing toward the inward source.

problem of beam steering has implemented interferometric feedback on every element, for example [21].

In this paper, we show how to establish multiple power-optimal orthogonal channels (or "communications modes" [14]) through arbitrary linear scatterers without measuring the wave field or the transmission matrix, without any calculations, without nonlinear optical materials, without moving parts, without calibration of the optical devices, and without fundamental splitting or combining loss. The method can be viewed as an automatic physical implementation of multiple-channel SVD.

In Section II, we discuss the simplest case of finding the optimum single channel from a simple source. In Section III, we extend this to optimizing both the transmitter and receiver ends. While some aspects of the devices in Sections II and III could be accomplished by other means such as phase conjugation [18], [19], the optimization of multiple optical channels simultaneously without fundamental splitting and/or combining loss, as discussed in Section IV, is apparently unique to this approach. We draw conclusions in Section V.

II. Single-Ended Single-Channel Optimization

To describe how this approach works, consider first the simple free-space situation in Fig. 1, shown for a 1-D array of grating coupler elements for graphical simplicity. (2-D versions of the self-aligning universal beam coupler in Fig. 1 are discussed explicitly in [20], and those could also be employed here.)

A beam from an external "inward" source shines onto the grating couplers. The couplers are the inputs to a self-aligning universal beam coupler [20], which adjusts the Mach–Zehnder interferometer (MZI) couplers MZ1–MZ4, based on signals from the photodetectors D1–D3, so as to couple essentially all the light from the grating couplers into one single-mode input/output waveguide. That light emerges as indicated by the orange-colored "inward wave" arrow from the single-mode input/output waveguide at the bottom right of Fig. 1.

The operation of the self-aligning coupler is described in detail in [20]. Briefly, in the present example, light coupled in through grating coupler G4 passes through MZ4, which is operated only as a phase shifter; phase shift in an MZI can be set by the common mode drive of the phase shifters in its two arms. (A simple phase shift element could also be substituted for MZ4). That phase shifter is adjusted to minimize the total detected power in detector D3, a process that sets the field contributions from both G4 and G3 to be in antiphase. Then we adjust what we can call the "reflectivity" of MZ3 (through the differential drive of the phase shifters in the MZI arms) to minimize the power in D3 again (ideally now to zero power because the field cancellation will now be complete). (By "reflectivity" here we mean effectively how the incident power in one input arm of the MZI interferometer is split between the two output arms, in the spirit of operating the MZI device as a variable beamsplitter [20]; we do not mean back-reflection from the interferometer, which we presume here to be effectively zero in all cases.) Next, the power in D2 is minimized similarly, first through the common mode drive of MZ3 to set phase and then through the differential drive of MZ2, and so on for any successive detectors and MZI couplers. The net result of this whole process is to end up with settings of the MZI such that there is negligible or zero power into any of the detectors, and so all the "inward wave" power now emerges from the single-mode input/output waveguide. If we added a small intensity modulation or some other modulation identifier on the inward beam and then in detectors D1–D4 we looked only for signals with that modulation, then we could improve the discrimination of the desired signal from other background light.

So far, we have merely summarized the operation of the self-aligning universal mode coupler [20]. Now, however, we shine a "backward wave" into the single-mode input/output waveguide, as shown by the red arrow at the bottom of Fig. 1. This wave will experience the same phase delays and amplitude splitting as the inward wave did as it propagates back to the grating couplers. We can think of the set of (complex) amplitudes in the single modes in the waveguides W1–W4 connected to the grating couplers as being a supermode of those single-mode guides. The net result of this process is that the backward wave going into the grating couplers in W1–W4 represents the phase conjugate [16], [17] of the inward wave in W1–W4 coming from the grating couplers.

To understand this backward behavior more intuitively, note first that the self-aligning universal mode coupler will adjust its internal phase delays and reflectivities so that all the "inward" waves add in phase by the time they get to the single-mode

input/output guide. Since, in Fig. 1, an inward (orange-colored) phase front will arrive last at the grating coupler G1, this path will be set during the self-alignment to have the shortest phase delay. When running the device backward (as in the red-colored arrows and phase fronts), the phase front will therefore get first to G1, so it will launch first as required, so as to get the backward phase fronts curved as in the red lines. We can argue similarly for the phase delays to the other grating couplers. The net result is to generate the red-colored phase fronts going back toward the original inward source (at least approximately so).

Of course, this device is only sampling the phase fronts at discrete points or regions (in Fig. 1, four averaged points corresponding to the four grating couplers). But, in the spirit of Huygens' principle (see [22] for a recent discussion), the wavelets (sketched as dashed lines) from these sources construct their best representation of the red-colored backward-propagating phase fronts. The number of regions or waveguides we want in a given device depends first on the number of orthogonal channels we want, and second on how complex those channels are (or, equivalently, how many degrees of freedom we need to distinguish one channel from another); this point is discussed in a greater detail in [23] and [24]. We also note that there are various other ways of implementing the self-aligning universal beam coupler in Fig. 1, as discussed in [20]. These include the addition of lenslets in the optical case, and in the microwave case, the use of antennas instead of the grating couplers.

The device of Fig. 1, as it stands, is already useful for establishing a backward channel to this inward source, a channel that could be used for communicating efficiently back to that source in a bidirectional link, for example. Such a channel could also be used for remote power delivery from the backward wave source to some appropriate power detector at the inward wave source. Alternatively, by partially back-reflecting the inward power leaving the single-mode guide so that this reflected power gives a backward wave (i.e., the beam represented by the thick red arrow could be formed from some reflected power from the beam represented by the thick orange arrow), the optimized bidirectional channel could be created without the need for another source for the backward wave. Conceivably, in that case, the detected power in the self-aligning beam coupler could be used to power that entire device and its feedback loop electronics, allowing a remote element with no local power source for, e.g., environmental sensing or biological applications. Note, too, that an approach like this will also work even if there is a scattering object in the way between the inward source and the self-aligning universal beam coupler, as is well known for phase conjugate optics [16]–[19].

We could also run the device shown in Fig. 1 starting with the red-colored source into the single-mode input/output waveguide as the optical source, leading to a beam propagating out toward the "inward source" position; the scattering off that inward "source" could constitute the backward orange-colored wave that we would then use to optimize the red-colored beam so that it focuses more effectively onto the "inward source" position. Such an operation mode could also be useful for addressing remote sensors, including power delivery to them. If at the inward "source" we impose some modulation of its scattering and we look in detectors D1–D4 for signals with that modulation, we can improve our ability to lock our channel onto this particular scatterer. Since the feedback sequence in this self-aligning beam coupler can be left running continuously [20], this approach could also be used even if the inward source and the self-aligning universal beam coupler are moving relative to one another, thus allowing this bidirectional channel to "track" relative movement.

The inward and backward waves could be at the same frequency here, or they could be at different frequencies or with finite bandwidths of sources provided only that the relative phase delays for the different frequencies or bandwidth range in the different optical paths from grating couplers to the single-mode input/output waveguide are all substantially similar within the frequency or wavelength range of interest. Keeping all the optical path lengths from the different grating couplers to the single-mode input/output waveguide approximately equal is desirable for keeping such approximate frequency independence of the relative phase delays in the different paths.

Note that, though the same function as described here could be achieved by measuring the inward wave amplitude and phase and then calculating and applying appropriate drive to calibrated Mach–Zehnder devices, the present approach avoids such measurement, calibration, and calculations. Optical phase conjugation approaches to related problems are well known [16]–[19]; this present approach can be regarded as implementing phase conjugation but without the need for nonlinear optical materials and with the desired input or output being in a convenient, waveguide form.

III. Double-Ended Single Channel Optimization

The approach as shown in Fig. 1 does not itself incorporate any optimization of the inward source form. Such optimization could result in better coupling efficiencies overall in such a bidirectional system. Fig. 2 shows a version in which self-aligning beam couplers are used at both ends of the link.

An interesting question now is to understand the nature of the wave that will form in the case of Fig. 2 if two self-aligning universal mode couplers are running one into the other. To understand this mathematically, we can use the result from [15] that, for essentially any linear operator relating waves or sources in one ("left") space to waves in another ("right") space, we can perform the SVD of the resulting coupling operator to define two complete orthonormal ("mode-converter" or "communication mode") basis sets, one set $|\phi_{Lm}\rangle$ for the "left" space and a corresponding set $|\phi_{Rm}\rangle$ for the "right" space. Here, for example, we could think of the "left" ("right") space as being the waves on the surface of the grating couplers on the left (right). It may be mathematically cleaner and simpler, however, to consider functions in the "left" mathematical space as being the set of amplitudes of the "red" single modes in the waveguides going into the grating couplers (i.e., a supermodes of those waveguides) on the "left" side (as in waveguides W1–W4 in Fig. 1), and the "right" space as being correspondingly the set of amplitudes of the "red" single modes (or the supermode) in the waveguides coming out of the grating couplers on the "right"

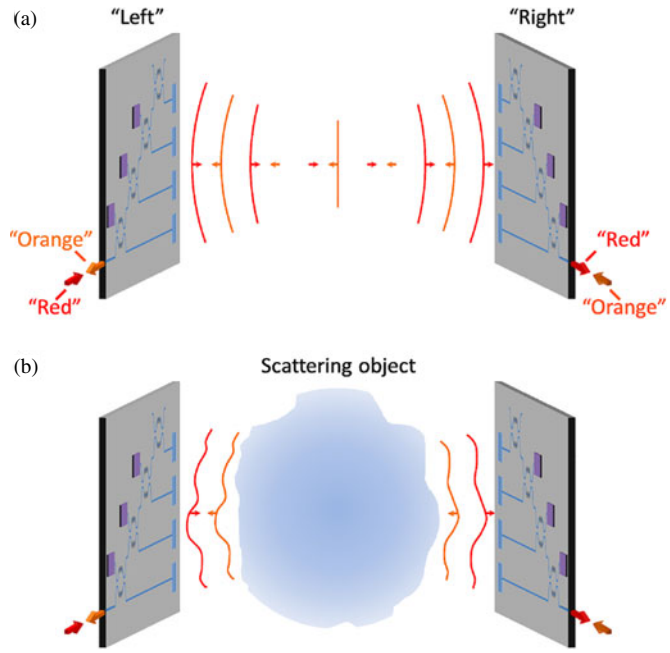

Fig. 2. Illustration of two single-channel self-aligning universal mode couplers used at the two ends of a link. (a) Through free space. (b) With a scattering object.

side. (In these implementations, it is actually these supermodes that are strictly the orthogonal modes in the system, and not the waves at the grating coupler surfaces.)

For the example structures in Fig. 2, any function in either of these mathematical spaces is therefore representable as a four (complex)-element vector (at least if we consider monochromatic fields for the moment); in general, with similar systems each with M grating couplers and waveguides on each side, the corresponding basis (supermode) functions would be M (complex)-element vectors. With the mathematical spaces chosen this way, the coupling "device" operator D [15] between the "left" space and the "right" space is an $M \times M$ matrix.

The fact that we can essentially always perform the SVD of D [15] means not only that we could obtain the two sets $|\phi_{Lm}\rangle$ and $|\phi_{Rm}\rangle$, each comprising M different vectors, but also that these vectors are connected one by one with specific (field) coupling strengths given by the singular values s_m. That is, for each of the M different orthogonal "left" functions (or supermodes) $|\phi_{Lm}\rangle$,

$$\mathsf{D}\,|\phi_{Lm}\rangle = s_m\,|\phi_{Rm}\rangle\,. \tag{1}$$

Hence, at least mathematically, we can have M orthogonal channels (or, in a generalized sense, communications modes [14]), with the orthogonal "left" output supermodes $|\phi_{Lm}\rangle$ giving orthogonal "right" input supermodes $|\phi_{Rm}\rangle$, each with corresponding amplitude s_m. Note that these sets of functions $|\phi_{Lm}\rangle$ and $|\phi_{Rm}\rangle$ are each mathematically complete for their respective spaces.

Suppose, then, that we start out with some arbitrary setting of the "left" set of MZIs, and shine a "red" beam into the single-mode input/output waveguide on the left. We will therefore have some output supermode $|\phi_L{}^{(1)}\rangle$ going to the "left" grating couplers in the "left" waveguides, which we can expand in the complete set $|\phi_{Lm}\rangle$, i.e.,

$$|\phi_L^{(1)}\rangle = A_L^{(1)} \sum_{m=1}^{M} a_m\,|\phi_{Lm}\rangle \tag{2}$$

where $A_L^{(1)}$ is a factor related to the power in the "red" beam, and the coefficients a_m result from the arbitrary initial setting of the MZIs. Now we send this wave out through the "left" grating couplers and the intervening space (which might include some scattering object) to the "right" grating couplers. The resulting supermode set of amplitudes in the waveguides coming out of the "right" grating couplers is, when expanded on the set $|\phi_{Rm}\rangle$,

$$|\phi_R^{(1)}\rangle = \mathsf{D}|\phi_L^{(1)}\rangle = A_L^{(1)} \sum_{m=1}^{M} s_m\,a_m\,|\phi_{Rm}\rangle. \tag{3}$$

Now, we run the self-alignment process in the "right" self-aligning beam coupler, fixing the resulting "right" MZI settings to optimally couple this wave out of the single mode waveguide on the right, as shown with the outward red arrow in Fig. 2.

Next, we turn on the backward "orange" light source, generating a backward propagating wave. We presume that the optical system through the grating couplers and the intervening space or scatterer is made from materials with symmetric permittivity and permeability tensors, as is nearly always the case in optical materials in the absence of static magnetic fields, and that this system is not time varying, or that any time variation is negligible over the timescales of interest. As a result, this optical system shows reciprocity. Because of that reciprocity, we know that if a given supermode from the "left" waveguides propagated forward through the system to one particular "right" supermode, without scattering to any of the other "right" modes, and with a complex transmission factor s_m, then the same supermode going backward (i.e., in a phase-conjugated fashion) will also proceed without scattering to other backward modes, and will have the same complex transmission factor s_m (i.e., the same magnitude of field transmission and the same phase pick-up) going backward. Hence, each basis supermode will return to the original "left" device, in a phase-conjugated form, with an amplitude $s_m^2\,a_m\,\mathrm{A}_R^{(1)}$, where now $A_R^{(1)}$ is a factor related to the power in the "orange" beam.

Next, we run the self-alignment process in the "left" self-aligning beam coupler. The "red" beam will now lead to some output that is the phase conjugate of the beam that was arriving from the right, i.e.,

$$|\phi_L^{(2)}\rangle = A_L^{(2)} \sum_{m=1}^{M} s_m^2\,a_m\,|\phi_{Lm}\rangle \tag{4}$$

where $A_L^{(2)}$ is some factor related to the "red" beam power. Going round this loop again—i.e., running the self-alignment process in the "right" self-aligning beam coupler, using the "orange" light source to send the beam back again, and running the "left" self-alignment process once more—will lead to some

"red" output

$$|\phi_L^{(2)}\rangle = A_L^{(3)} \sum_{m=1}^{M} s_m^4 a_m |\phi_{Lm}\rangle . \quad (5)$$

We can see now that what is happening is that the communication mode with the largest singular value (i.e., field coupling strength) magnitude will progressively dominate over the other modes in the summation as these singular values s_m are raised to progressively higher powers every time we go round this loop.

Since the numbering of the communication modes here is up to us, we can always choose to number them by decreasing magnitude of s_m. So, regardless of the initial (presumably nonzero) strength (i.e., its coefficient a_1) of the mode with the largest singular value, eventually, after sufficiently many iterations of running the self-alignment processes on the "right" and "left" self-aligning beam couplers, the output will tend to the most strongly coupled mode.

Thus, this system in Fig. 2, when run with only local optimizations in the self-aligning beam couplers at each side, will find the most strongly coupled communication mode between the waveguides in these two devices, regardless of the form of the scattering between the devices (and regardless of the form of the grating couplers or other wave coupling devices in and out of the waveguides). This whole process is, of course, strongly analogous to the build-up of the mode with the highest gain in a laser resonator; the analogy between communications modes and the laser modes of a resonator with phase conjugate mirrors at both ends has been pointed out for the simple free-space case [14], and we have generalized this result here. Indeed, the use of phase conjugate mirror pairs has been proposed and demonstrated for performing one such optimized coupling [18], [19]. Again, our approach avoids finding appropriate nonlinear materials and delivers the beams in a convenient single mode form at the either end. This method is also mathematically similar in spirit to the power iteration or the von Mises method of finding the largest eigenvalue and eigenvector of a matrix mathematically [25].

IV. Double-Ended Multiple Channel Optimization

The devices in Figs. 1 and 2 only show a single spatial channel associated with a given self-aligning beam coupler. Following the previous discussions [20] of related devices, we can also make versions of such devices that can handle multiple orthogonal modes simultaneously. Because of these multiple channels, the devices go beyond the capabilities of simple phase conjugation approaches [18], [19] and the typical use of power iteration methods in mathematics [25], which is to find only the largest eigenvalue and eigenvector, and they avoid the fundamental splitting loss of previous measure-and-calculate multiple channel optical approaches [10].

Fig. 3 shows a version of the device of Fig. 2, but configured with additional MZIs and detectors. The various detectors in Fig. 3 are presumed to be mostly transparent [20], sampling only enough of the beam power passing through them to give enough signal to run the feedback loops. In general, with such devices, with M input couplers, we can make a device that can handle M orthogonal modes simultaneously. The device in

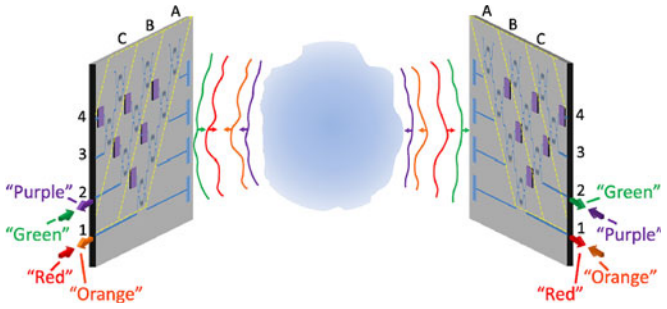

Fig. 3. Illustration of coupling multiple orthogonal modes simultaneously. The yellow dashed diagonal lines indicate different "rows" of the Mach–Zehnder interferometers and detectors used to set the different orthogonal modes.

Fig. 3 can handle four orthogonal modes, and beams and waves are sketched explicitly for two orthogonal modes.

To set up two orthogonal channels in the device shown in Fig. 3, we could first proceed as for the device shown in Fig. 2, turning on the "red" and "orange" beams and adjusting the MZI settings using the signals from their corresponding detectors (now the interferometers and detectors in the diagonal row A of Fig. 3) as described above to establish the first optimized channel, with corresponding supermodes $|\phi_{L1}\rangle$ and $|\phi_{R1}\rangle$ in the waveguides leading to the grating couplers on the left and the right, respectively.

A key point to note now is that, regardless of the settings of the MZIs in row B, shining light into waveguide 2 (e.g., the "green" beam on the left or the "purple" beam on the right) leads to "green" supermodes in the waveguides connected to the grating couplers that are orthogonal to the supermodes $|\phi_{L1}\rangle$ and $|\phi_{R1}\rangle$, respectively. None of the power shining into waveguide 2 on either side gets to waveguide 1 on the other side. The supermodes excited in the waveguides on the left by shining the "green" beam into waveguide 2 are guaranteed always to be orthogonal to the supermode $|\phi_{L1}\rangle$; similarly, the supermode in the waveguides on the right by shining in the "purple" beam into waveguide 2 on the right is necessarily orthogonal to $|\phi_{R1}\rangle$.

So, now, leaving the devices in rows A fixed at the settings we just established for the optimized "red/orange" channel 1, we can run the same kind of optimization procedure for the devices in row B with the "green" and "purple" beams that we originally ran for the devices in row A with the "red" and "orange" beams. This process leads to supermodes $|\phi_{L2}\rangle$ and $|\phi_{R2}\rangle$ that are orthogonal, respectively, to the supermodes $|\phi_{L1}\rangle$ and $|\phi_{R1}\rangle$. (Note that the labels "red", "orange", "green," and "purple" need not refer to actual colors of light beams—indeed, all the beams here can be of exactly the same wavelength or frequency; these labels are for descriptive and graphical clarity only.)

Now we have established two orthogonal channels. Light shining into input/output waveguide 1 on the left appears only at input/output waveguide 1 on the right, and similarly for input/output waveguide 2. We can repeat a similar procedure for any remaining rows of devices. In our example here, we have only one remaining row to set, which we can use to establish a third orthogonal channel, now from input/output waveguide 3

on one side to input/output waveguide 3 on the other. Automatically, we also establish the final orthogonal channel—shining light now into waveguide 4 on either side leads also only to light coming out of waveguide 4 on the other side. In general, to establish M orthogonal channels, we need to run our optimization process on $M-1$ rows of interferometers and detectors.

Hence, we have now established all the independent orthogonal communication mode channels between one side and the other, regardless of the scattering medium between the two sides, as long as it is reciprocal and does not change significantly during the timescale of the optimization process. These channels are in order of decreasing coupling strength (or magnitude of the singular values). We can use the resulting settings of the various phase shifters and/or beamsplitters in the devices on the left and the right in Fig. 3 to formally measure the device or coupling operator between the left and the right (see Appendix A). Note that attempting to pass limits on the number of strongly coupled channels as set by diffraction or its SVD generalization [14] will result in a fall-off in these coupling strengths; indeed, we can expect a sum rule on the squared modulus of these singular values [14]. This point is discussed in Appendix B.

If we have no other way of distinguishing between the various beams in the detectors, the scheme described here does require that, in setting the device, we first work with the "red" and "orange" beams, with the other beams turned OFF, and only progressively turn ON the light in the other waveguides, holding fixed the interferometer settings in preceding rows. This particular scheme cannot be left running continuously to optimize all the modes as the system changes (e.g., for relative movement of the two object or for changes in the scattering); to reoptimize the "red–orange" channel 1, we would need to turn OFF the other beams, for example.

There are, however, many ways we could effectively make the beams distinguishable in the signals they give in the detectors, as mentioned already briefly for the single-ended single-channel optimization in Section II. For example, we could impose different low frequency small modulations [20] of each of the sources of the beams labeled with different colors in Fig. 3. The feedback electronics connected to each row of detectors could then be programmed to look only for the corresponding modulation frequency (for example, using lock-in detection). Alternatively, some other identifying code could similarly be imposed on each of the beams, with corresponding decoders to pick out such identifiers. With such schemes, the different modes could all be optimized simultaneously with all the beams running, for example, by stepping through the optimizations of the modes one by one, in sequence from mode 1 upward, and continuing to cycle through all the modes in such a manner.

The use of heterodyne or homodyne detection approaches in the detectors could lead to very specific identification of channels (for example, finding channels within a very narrow frequency range relative to a local oscillator). For example, if we use a monochromatic red-colored beam from the left, and then partially reflect it back into the input/output waveguide on the right to function as the orange-colored beam in the schemes in Figs. 2 or 3, then, by mixing with portions of the original red beam, we have the option of homodyne detection in the detectors on the left, which could allow very specific discrimination against any other signals of even slightly different frequencies incident on the grating couplers on the left, e.g., from the environment. Imposing a modulation, e.g., from a modulator inserted in the input/output waveguide just before the partial back-reflection on the right, would allow heterodyne detection on the left; looking in the detector outputs on the left for the desired frequency sideband imposed by the modulation on the right would also allow discrimination against any direct backscatter from the scatterer or from optical components in the path of the original "red" beam from the left back into the left self-aligning beam coupler; only the actual beam from the device on the right would have this side-band present.

V. Conclusion

We have presented an approach that allows two objects to establish multiple optimal channels for communication in the presence of arbitrary scattering or loss in different physical modes. The approach is based only on local feedback loops minimizing detector signals by progressively adjusting parameters of beamsplitters, two-beam interferometers, or phase shifters. Importantly, multiple optimized orthogonal spatial channels can be set up and maintained simultaneously, without any fundamental splitting loss. The different modes can be optimized sequentially by cycling through the optimizations of them. The mathematics of the resulting optimized communications modes is analogous to the formation of laser modes in a cavity with two phase-conjugate mirrors [18], though no laser action in the device is required. Our approach avoids the necessity of finding appropriate nonlinear optical materials for phase conjugation at power levels and/or wavelengths of interest and conveniently separates out the modes of interest to individual single modes at either end. More deeply, though phase conjugation can perform several self-alignment or tracking functions for a single channel [19], our approach allows multiple orthogonal modes to be established and/or tracked simultaneously.

There are many possible applications of this approach. It can be used to establish multiple orthogonal spatial channels through media such as multimode optical fibers, free space, scattering objects (such as biological tissue), atmospheric turbulence, and turbulence in fluids. Such an approach could also allow imaging of multiple pixels simultaneously through such media, even when the scattering is substantially different for different pixels. It can automatically align multiple channels for free-space optical interconnects even as the physical positions drift. It can find optimum modes for communicating into and out of remote sensors or communication devices, including possibly finding the sensors on the basis of their backscattered signal. It can be used for optimal power delivery to remote devices, including possibly external powering of sensors, while simultaneously establishing communication channels. It can steer multiple beams and track multiple moving objects while retaining optimized communications and/or power delivery, allowing a kind of active lidar that could follow detected target objects. Modulation of a launched or backscattered signal from a remote device and/or the use of homodyne or heterodyne detection together with this approach

could allow optimization of very specific channels, while rejecting environmental interference and backscattering from the intervening medium.

The method could be extended straightforwardly to handle different polarizations of beams, including scattering between polarizations, by the "representation converter" approach given in [24]; the two orthogonal polarizations in each spatial mode in the propagation medium are separated to different spatial channels inside the self-aligning couplers (we convert the representation from polarization modes to spatial modes); this doubles the number of spatial channels or waveguides inside the couplers, but the self-aligning process otherwise proceeds as before. In principle at least, such an approach can also handle different spectra or pulse shapes by a related representation conversion, now from frequency or time degrees of freedom to spatial modes [24], though the required frequency converters or time-multiplexers would currently be difficult in practice.

We have shown here specific examples using MZIs in a planar optical platform as an illustration. Other approaches that can allow controllable reflectivity and phase in wave elements could exploit the same overall approach [20], [24], and different technologies could be exploited in other wave domains, such as microwaves, where many corresponding components are known [26]. The grating couplers discussed here also represent only one way of coupling between free-space or multimode fibers and individual waveguides; photonic lanterns [27]–[29] offer another interesting approach for such couplings.

Though MIMO methods are available at radio [1]–[4] and optical [10] frequencies based on measurement of the transmission operator through the communications medium and calculation of resulting optimized channels, the present method avoids such measure-and-calculate approaches and any power dissipation associated with them. It also avoids the power splitting loss of previous optical multichannel MIMO schemes [10]. The avoidance of any measurement on the signal itself at rates corresponding to the information bandwidth being transmitted means that this method is not restricted in bandwidth by those measurements. The absence of measurement on the signal means that the quantum state of the optical signal does not suffer from state collapse from those measurements, allowing this scheme to be used in quantum communications and information processing.

In conclusion, the novel method presented here offers a physical method of establishing optimal orthogonal channels through arbitrary linear scatterers or communication media based on the minimization of the detected power in local feedback loops, for low-power, low-loss, multiple-channel classical and quantum systems.

Appendix A

Measuring the Coupling Operator

Though the method here does not require any calibration of the phase-shifters or beamsplitters, if those are calibrated, then by reading off the values of them once we have self-aligned the entire system and performing some power coupling strength measurements, we can deduce a measurement of the device or coupling operator between the two sides.

The settings of the first row(s) of beamsplitters directly allow us to extract the functions associated with the largest singular value or coupling strength [24]. The settings in the subsequent rows allow us to calculate the corresponding functions associated with the progressively smaller singular values or coupling strengths; in those cases, we have to use our knowledge of the settings of devices in previous rows to allow us formally to transform back to deduce the corresponding functions in the waveguides connected to the grating couplers or other coupling devices, as discussed in [24]. One simple way to view this [24] is to imagine shining beams into the waveguides at the far left in Fig. 3. The beams that we get at the waveguides connected to the grating couplers or other output devices can be readily calculated from the known settings of the phase shifters and/or beamsplitters in the device, and these can be viewed as the singular value decomposition functions for this "transmit" side of the system. Similarly, if we imagine shining beams "back" into the waveguides at the far right in Fig. 3, the resulting beams we would generate coming "left-wards" from the right hand side would be the phase conjugates of the "received" singular value decomposition functions. Hence from these sets of functions, we know the form of the singular value decomposition.

We can then also measure the power coupling efficiencies from one side to the other for each of these beams (by measuring the output power on one side for a given waveguide for a given input power in the corresponding waveguide on the other side); these efficiencies are the squares of the singular values. Hence, at least within phase factors for each channel or communications mode, we know the complete singular value decomposition of the device (or coupling) operator D, at least up to the dimensionality M of our system.

Appendix B

How Many Strong Channels?

When working with a communications system, it is generally useful to know how many well coupled channels we can have. The approach here can give simple insight.

Suppose first that, before any optimization of the device, we shine a beam of unit power into the first waveguide on the far left in Fig. 3. We can think of this as giving rise to some unit power "right-ward" output wave from the device on the left in Fig. 3 of $|\phi_{L1}\rangle$. This will give some wave arriving into the device on the right of

$$|\phi_{R1}\rangle = \mathsf{D}\,|\phi_{L1}\rangle\,. \tag{6}$$

The total power in this beam, which is the sum of the powers in all of the output waveguides on the far right, is

$$P_1 = \langle\phi_{R1}\mid\phi_{R1}\rangle = \langle\phi_{L1}|\,\mathsf{D}^\dagger\mathsf{D}\,|\phi_{L1}\rangle\,. \tag{7}$$

We can repeat this experiment for all M different waveguides on the far left. Adding up all the corresponding powers for each such experiment, we obtain

$$S = \sum_{i=1}^{M} P_i = \sum_{i=1}^{M} \langle\phi_{L1}|\,\mathsf{D}^\dagger\mathsf{D}\,|\phi_{L1}\rangle \equiv \mathrm{Tr}\left(\mathsf{D}^\dagger\mathsf{D}\right). \tag{8}$$

Now, the trace (Tr) of a linear operator (or matrix) is independent of the (complete) basis used to represent it. What this means here is that it does not matter how the various phase shifters and/or beamsplitters are set up in the devices on the right and the left in Fig. 3; the sum S of the power efficiencies measured this way will always be the same. (This kind of sum rule was noted in [14], where it allows us to define the diffraction limit in optics in a generalized way.)

So, we could imagine performing the experiment as described here to measure S, and then starting the optimization procedure. For each channel that we set up this way, which of course couples power from one waveguide on the left to one waveguide on the right, we can note the power efficiency. As we perform the optimization for each successive channel, we note the running total of these efficiencies. As that running total comes nearer to the number S we have already measured, we can see whether we have enough strength left to allow another well-coupled channel by whatever criterion we choose for minimum useful power coupling strength. Once we have insufficient power coupling strength left, we can stop trying to find any more well-coupled channels because there will be no more.

ACKNOWLEDGMENT

I am pleased to acknowledge stimulating and informative conversations with Joseph Kahn and Robert Thomson. I am grateful for the hospitality of Strathclyde University and Heriot-Watt University where portions of this work were completed, and for the support of the Carnegie Trust for the Universities of Scotland through the Carnegie Centenary Professorship during that visit.

REFERENCES

[1] C.-N. Chuah, J. M. Kahn, and D. Tse, "Capacity of multi-antenna array systems in indoor wireless environment," in *Proc. Globecom 1998*, 1998, vol. 4, pp. 1894–1899.

[2] G. J. Foschini and M. J. Gans, "On limits of wireless communications in a fading environment when using multiple antennas," *Wireless Pers. Commun.*, vol. 6, pp. 311–335, 1998.

[3] D. P. Palomar, J. M. Cioffi, and M. A. Lagunas, "Joint Tx-Rx beamforming design for multicarrier MIMO channels: A unified framework for convex optimization," *IEEE Trans. Signal Process.*, vol. 51, no. 9, pp. 2381–2401, Sep. 2003.

[4] L. Hanlen and M. Fu, "Wireless communication systems with-spatial diversity: A volumetric model," *IEEE Trans. Wireless Commun.*, vol. 5, no. 1, pp. 133–142, Jan. 2006.

[5] S. M. Popoff, G. Lerosey, R. Carminati, M. Fink, A. C. Boccara, and S. Gigan, "Measuring the transmission matrix in optics: An approach to the study and control of light propagation in disordered media," *Phys. Rev. Lett.*, vol. 104, p. 100601, 2010.

[6] T. Čižmár and K. Dholakia, "Shaping the light transmission through a multimode optical fibre: Complex transformation analysis and applications in biophotonics," *Opt. Exp.*, vol. 19, pp. 18871–18884, 2011.

[7] S. Bianchi and R. Di Leonardo, "A multi-mode fiber probe for holographic micromanipulation and microscopy," *Lab Chip*, vol. 12, p. 635, 2012.

[8] R. N. Mahalati, D. Askarov, J. P. Wilde, and J. M. Kahn, "Adaptive control of input field to achieve desired output intensity profile in multimode fiber with random mode coupling," *Opt. Exp.*, vol. 20, pp. 14321–14337, 2012.

[9] A. P. Mosk, A. Lagendijk, G. Lerosey, and M. Fink, "Controlling waves in space and time for imaging and focusing in complex media," *Nature Photon.*, vol. 6, pp. 283–292, 2012.

[10] R. Ryf, S. Randel, A. H. Gnauck, C. Bolle, A. Sierra, S. Mumtaz, M. Esmaeelpour, E. C. Burrows, R.-J. Essiambre, P. J. Winzer, D. W. Peckham, A. H. McCurdy, and R. Lingle Jr., "Mode-division multiplexing over 96 km of few-mode fiber using coherent 6 × 6 MIMO processing," *J. Lightw. Technol.*, vol. 30, pp. 521–531, 2012.

[11] E. J. Bond, X. Li, S. C. Hagness, and B. D. Van Veen, "Microwave imaging via space-time beamforming for early detection of breast cancer," *IEEE Trans. Antennas Propag.*, vol. 51, no. 8, pp. 1690–1705, Aug. 2003.

[12] F. Vignon and M. R. Burcher, "Capon beamforming in medical ultrasound imaging with focused beams," *IEEE Trans. Ultrason., Ferroelectr., Freq. Control*, vol. 55, no. 3, pp. 619–628, Mar. 2008.

[13] M. Bertoro, C. De Mol, and E. R. Pike, "Linear inverse problems with discrete data—Part I: General formulation and singular system analysis," *Inverse Problems*, vol. 1, pp. 301–330, 1985.

[14] D. A. B. Miller, "Communicating with waves between volumes—Evaluating orthogonal spatial channels and limits on coupling strengths," *Appl. Opt.*, vol. 39, pp. 1681–1699, 2000.

[15] D. A. B. Miller, "All linear optical devices are mode converters," *Opt. Exp.*, vol. 20, pp. 23985–23993, 2012.

[16] P. Günter, "Holography, coherent light amplification and optical phase conjugation with photorefractive materials," *Phys. Reports*, vol. 193, pp. 199–299, 1982.

[17] A. Yariv, "Phase conjugate optics and real-time holography," *IEEE J. Quantum Electron.*, vol. QE-14, no. 9, pp. 650–660, Sep. 1978.

[18] S. Weiss, S. Sternklar, and B. Fischer, "Double phase-conjugate mirror: Analysis, demonstration, and applications," *Opt. Lett.*, vol. 12, pp. 114–116, 1987.

[19] A. S. Kuzhelev, A. E. Dudelzak, M. Maszkiewicz, D. Gratton, and L. Hotte, "Optical communications between moving transceivers using double phase-conjugate beam tracking," *Proc. SPIE*, vol. 5577, pp. 636–647, Dec. 20, 2004.

[20] D. A. B. Miller, "Self-aligning universal beam coupler," *Opt. Exp.*, vol. 21, pp. 6360–6370, 2013.

[21] T. K. Chan, M. Megens, B.-W. Yoo, J. Wyras, C. J. Chang-Hasnain, M. C. Wu, and D. A. Horsley, "Optical beamsteering using an 8 × 8 MEMS phased array with closed-loop interferometric phase control," *Opt. Exp.*, vol. 21, pp. 2807–2815, 2013.

[22] D. A. B. Miller, "Huygens's wave propagation principle corrected," *Opt. Lett.*, vol. 16, pp. 1370–1372, 1991.

[23] D. A. B. Miller, "How complicated must an optical component be?" *J. Opt. Soc. Am. A*, vol. 30, pp. 238–251, 2013.

[24] D. A. B. Miller, "Self-configuring universal linear optical component," *Photon. Res.*, vol. 1, pp. 1–15, 2013.

[25] R. von Mises and H. Pollaczek-Geiringer, "Praktische verfahren der gleichungsauflösung," *ZAMM—Zeitschrift für Angewandte Mathematik und Mechanik*, vol. 9, pp. 152–164, 1929.

[26] K. Chang (ed.), *Handbook of RF/Microwave Components and Engineering*. Hoboken, NJ, USA: Wiley, 2003.

[27] D. Noordegraaf, P. M. Skovgaard, M. D. Nielsen, and J. Bland-Hawthorn, "Efficient multi-mode to single-mode coupling in a photonic lantern," *Opt. Exp.*, vol. 17, pp. 1988–1994, 2009.

[28] R. R. Thomson, T. A. Birks, S. G. Leon-Saval, A. K. Kar, and J. Bland-Hawthorn, "Ultrafast laser inscription of an integrated photonic lantern," *Opt. Exp.*, vol. 19, pp. 5698–5705, 2011.

[29] N. K. Fontaine, R. Ryf, J. Bland-Hawthorn, and S. G. Leon-Saval, "Geometric requirements for photonic lanterns in space division multiplexing," *Opt. Exp.*, vol. 20, pp. 27123–27132, 2012.

David A. B. Miller (M'83–F'95) received the Ph.D. degree in physics from Heriot-Watt University, Edinburgh, U.K., in 1979. He was with Bell Laboratories from 1981 to 1996, as a Department Head from 1987. He is currently the W. M. Keck Professor of Electrical Engineering and Co-Director of the Stanford Photonics Research Center at Stanford University, Stanford, CA, USA. He was the President of the IEEE Lasers and Electro-Optics Society in 1995. His research interests include physics and devices in nanophotonics, nanometallics, and quantum-well optoelectronics, and fundamentals and applications of optics in information sensing, switching, and processing. He has published more than 260 scientific papers and the text *Quantum Mechanics for Scientists and Engineers* (Cambridge, U.K.: Cambridge Univ. Press, 2008), and holds 69 patents. He has received numerous awards. He is a Fellow of the Optical Society of America (OSA), the American Physical Society (APS), the Royal Society, and the Royal Society of Edinburgh, and is a member of the National Academy of Sciences and the National Academy of Engineering.